CHEMISTRY OF MATERIALS
Article

*Chem. Mater.* **2009,** *21,* 5079–5087 5079
DOI:10.1021/cm901618m

# Tuning the Grain Size and Particle Size of Superparamagnetic $Fe_3O_4$ Microparticles

Shouhu Xuan,[†] Yi-Xiang J. Wang,[‡] Jimmy C. Yu,[†] and Ken Cham-Fai Leung*,[†]

[†]*Center of Novel Functional Molecules, Department of Chemistry, The Chinese University of Hong Kong, Shatin, NT, Hong Kong SAR, and* [‡]*Department of Diagnostic Radiology and Organ Imaging, Prince of Wales Hospital, The Chinese University of Hong Kong, Shatin, NT, Hong Kong SAR*

*Received June 12, 2009. Revised Manuscript Received September 28, 2009*

Secondary structural, superparamagnetic $Fe_3O_4$ microparticles with an average diameter of 280 nm have been successfully synthesized by using a one-step hydrothermal method. The size of the primary nanograins has been controlled from 5.9 to 21.5 nm by varying the sodium acrylate/sodium acetate weight ratios. The magnetic properties of the $Fe_3O_4$ microparticles have been characterized at room temperature, whereas the saturation magnetization values of the $Fe_3O_4$ microparticles increase with increasing grain sizes. Magnetic resonance imaging reveals that $Fe_3O_4$ microparticle with larger grain size yields higher molar $T_2$ relaxation rate. A plausible growth mechanism of the particles is proposed, and the role of sodium acrylate and sodium acetate for tuning the grain size of the particles has been discussed. Additionally, the size of the secondary structural $Fe_3O_4$ particles can also be continuously controlled from 6 to 170 nm by varying the volume ratio of ethylene glycol/diethylene glycol in a bisolvent system. The described method presents the synthesis of secondary structural nanomaterials with tunable sizes, grain sizes, and different magnetic responses.

## 1. Introduction

The cubic inverse spinel structured $Fe_3O_4$ is an attractive material for essential applications such as ferrofluids, catalysts, biological assays, chemical sensors, and electrophotographic developers[1] because of their intrinsic magnetic features combined with the nanosize and surface effects. The structural and physicochemical properties of nanomaterials are of a great extent associated with the average particle size, particle shape, crystal order, surface characteristics, and presence or absence of bonded molecules.[2] In the case of magnetic properties for $Fe_3O_4$, it has been shown that the magnetic properties not only strongly depend on the particle size and surface but also on the degree of particles' crystallinity.[3] When the size of the $Fe_3O_4$ nanoparticle decreases to its critical value $r_c$, the magnet changes from a state with multiple magnetic domains to the one with a single domain. Such individual nanoparticle has a large, constant magnetic moment and behaves like a giant paramagnetic atom with a fast response to the externally applied magnetic field with negligible remanence (residual magnetizm) and coercivity (the field required to bring the magnetization to zero).[4]

After the discovery of this superparamagnetism property, it has been an increasing interest in the fabrication of $Fe_3O_4$ particles with superparamagnetic property at room temperature. Recently, several approaches have been explored to synthesize superparamagnetic $Fe_3O_4$ nanoparticles, which include chemical coprecipitation, thermal decomposition and/or reduction, micelle synthesis, hydrothermal synthesis, and laser pyrolysis techniques.[5] Besides these nanosized

*Corresponding author E-mail: cfleung@cuhk.edu.hk.

(1) (a) Raj, K.; Moskowitz, R. *J. Magn. Magn. Mater.* **1990**, *85*, 233–245. (b) Hu, A. G.; Yee, G. T.; Lin, W. B. *J. Am. Chem. Soc.* **2005**, *127*, 12486–12487. (c) Sen, T.; Sebastianelli, A.; Bruce, I. J. *J. Am. Chem. Soc.* **2006**, *128*, 7130–7131. (d) Martin, B. R.; Dermody, D. J.; Reiss, B. D.; Fang, M. M.; Lyon, L. A.; Natan, M. J.; Mallouk, T. E. *Adv. Mater.* **1999**, *11*, 1021–1025. (e) Huo, L.; Li, W.; Lu, L.; Cui, H.; Xi, S.; Wang, J.; Zhao, B.; Shen, Y.; Lu, Z. *Chem. Mater.* **2000**, *12*, 790–794. (f) Matijevic, P. E.; Hench, L. L.; Ulrich, D. B. In *Colloid Science of Composites System Science of Ceramic Chemical Processing*; Wiley: New York, 1986; p 463.

(2) (a) Chen, S. W.; Ingram, R. S.; Hostetler, M. J.; Pietron, J. J.; Murray, R. W.; Schaaff, T. G; Khoury, J. T.; Alvarez, M. M.; Whetten, R. L. *Science* **1998**, *280*, 2098–2101. (b) Schmid, G.; Baumle, M.; Geerkens, M.; Helm, I.; Osemann, C.; Sawitowski, T. *Chem. Soc. Rev.* **1999**, *28*, 179–185. (c) Murphy, C. J.; Jana, N. R. *Adv. Mater.* **2002**, *14*, 80–82. (d) Bakr, O. M.; Wunsch, B. H.; Stellacci, F. *Chem. Mater.* **2006**, *18*, 3297–3301. (e) Pasquato, L.; Pengo, P.; Scrimin, P. *Supramol. Chem.* **2005**, *17*, 163–171. (f) McIntosh, C. M.; Esposito, E. A.; Boal, A. K.; Simard, J. M.; Martin, C. T.; Rotello, V. M. *J. Am. Chem. Soc.* **2001**, *123*, 7626–7627. (g) Taton, T. A.; Mirkin, C. A.; Letsinger, R. L. *Science* **2000**, *289*, 1757–1760. (h) Puntes, V. F.; Gorostiza, P.; Aruguete, D. M.; Bastus, N. G.; Alivisatos, A. P. *Nat. Mater.* **2004**, *3*, 263–268. (i) Wenseleers, W.; Stellacci, F.; Meyer−Friedrichsen, T.; Mangel, T.; Bauer, C. A.; Pond, S. J. K.; Marder, S. R.; Perry, J. W. *J. Phys. Chem. B* **2002**, *106*, 6853–6863.

(3) (a) Roca, A. G.; Marco, J. F.; Morales, M. d. P.; Serna, C. J. *J. Phys. Chem. C* **2007**, *111*, 18577–18584. (b) Li, Z.; Sun, Q.; Gao, M. *Angew. Chem., Int. Ed.* **2005**, *44*, 123–126. (c) Morales, M. P.; Veintemillas-Verdaguer, S.; Montero, M. I.; Serna, C. J.; Roig, A.; Casas, L. I.; Martinez, B.; Sandiumenge, F. *Chem. Mater.* **1999**, *11*, 3058–3064.

(4) Jeong, U.; Teng, X.; Wang, Y.; Yang, H.; Xia, Y. *Adv. Mater.* **2007**, *19*, 33–60.

(5) (a) Harris, L. A.; Goff, J. D.; Carmichael, A. Y.; Riffle, J. S.; Harburn, J. J.; Pierre, T. G.; Saunders, S. M. *Chem. Mater.* **2003**, *15*, 1367–1377. (b) Peng, X.; Wickham, J.; Alivisatos, A. P. *J. Am. Chem. Soc.* **1998**, *120*, 5343–5344. (c) Mann, S.; Sparks, N. H. C.; Board, R. G. *Adv. Microb. Physiol.* **1990**, *31*, 125–181. (d) Si, S.; Li, C.; Wang, X.; Yu, D.; Peng, Q.; Li, Y. D. *Cryst. Growth Design.* **2005**, *5*, 391–393. (e) Veintemillas-Verdaguer, S.; Bomati-Miguel, O.; Morales, M. P. *Scr. Mater.* **2002**, *47*, 589–593.


Published on Web 10/13/2009

superparamagnetic particles, the efficient preparation of larger secondary structural superparamagnetic $Fe_3O_4$ particles (50−300 nm) have been attracted increasing attention because of their practical applications such as magnetic separation[6] and magnetic-targeted substrate delivery.[7] Generally, these secondary $Fe_3O_4$ particles are composed of small $Fe_3O_4$ nanocrystals. As-prepared superparamagnetic $Fe_3O_4$ particles are stable in solution and demonstrate rapid magnetic response to the externally applied magnetic field. Over the past decade, a number of approaches have been explored to synthesize secondary structural superparamagnetic $Fe_3O_4$ materials, which include spontaneous assembly,[8] cooperative assembly,[9] microemulsion templating,[10] and solvophobic interactions.[11] Compared to these two-step processes by assembling the presynthesized magnetic nanocrystals into uniform secondary structure, the direct one-step solution growth route to form the secondary structural $Fe_3O_4$ particles seems to be a simpler way, which is also economical for large-scale production.[12] Very recently, Yin and co-workers[13] reported a high-temperature hydrolysis method to grow monodisperse $Fe_3O_4$ nanoclusters. The approach has led to the synthesis of high-quality $Fe_3O_4$ particles with well-controlled size and shape. These as-prepared $Fe_3O_4$ particles can be assembled to photonic crystals in aqueous solution upon an externally applied magnetic field.

For particles of the same compositions and at a given temperature, the particle size is probably the most important parameter that rules their properties.[14] However, in the case of secondary structural materials from which all particles have a similar size, we ask ourselves how does the size of primary nanocrystals (or nanograins) influence their intrinsic property? For $Fe_3O_4$ nanocrystals, the size of primary nanocrystal determines if the overall particle is composed of a single magnetic domain or multiple domains. This will affect the magnetization (superparamagnetic or ferromagnetic) and the magnitude of the losses when they are exposed to an alternating magnetic field. The studies of such secondary structural $Fe_3O_4$ materials with grain size-dependent properties are rare because there are concerns and challenges in developing rational synthetic methodologies for the secondary structures with tunable grain sizes. Additionally, the size of the $Fe_3O_4$ particles is also very important accounting for their magnetic properties. There are only a few reports about fine control of $Fe_3O_4$ with particle sizes between 10 and 200 nm. Therefore, there is a pressing need to develop a novel method to construct secondary structural $Fe_3O_4$ particles with tunable primary nanograins sizes and secondary particles sizes through a one-step method as well as their systematical investigation of the grain size-dependence magnetic properties.

In this work, a modified solvothermal method[12b] was developed to construct a series of superparamagnetic $Fe_3O_4$ microparticles which comprised of tunable grain sizes, magnetic properties, and the size of the secondary structure. When $FeCl_3 \cdot 6H_2O$ was used as the sole iron source, the grain size and particle size of the secondary structures can be tuned rationally by using different amounts of ethylene glycol (EG), diethylene glycol (DEG), sodium acrylate (Na acrylate), and sodium acetate (NaOAc). All the secondary $Fe_3O_4$ microparticles products are superparamagnetic, whereas the saturation magnetization and $T_2$ relaxation values are directly related to the primary grain size from 5.9 to 21.5 nm. Additionally, we demonstrate that our approach can be extended to synthesize secondary structural $Fe_3O_4$ particles with diameters ranging from 6 to 280 nm by using a bisolvent method. Furthermore, this general approach is also applicable for the preparation of a series of ferrite particles. It is believed that this method can be applied to the synthesis of other magnetic materials with tunable size and grain size-dependent properties. The as-prepared superparamagnetic $Fe_3O_4$ particles with various grain sizes and particle sizes are water-soluble, which render them ideal candidates for practical applications such as magnetic separation, magnetic resonance imaging and drug delivery.

## 2. Experimental Section

**Materials.** Ferric chloride hexahydrate ($FeCl_3 \cdot 6H_2O$), sodium acrylate ($CH_2$=CHCOONa, Na acrylate), sodium acetate ($CH_3COONa$, NaOAc), ethylene glycol (EG), diethylene glycol (DEG), Poly(vinylpyrrolidone) (PVP, K30), branched polyethylenimine (PEI, 25 kDa) were obtained from Aldrich. All chemicals were of analytical grade and used without further purification. Deionized water was obtained from Barnstead RO pure system and was bubbled with high-purity nitrogen for at least 30 min before use.

**Synthesis of Monodisperse 280 nm $Fe_3O_4$ Particles with Tunable Grain Sizes of 5.9−13.5 nm.** $FeCl_3 \cdot 6H_2O$ (0.54 g), Na acrylate, and NaOAc were dissolved in EG (20 mL) under magnetic stirring. The obtained homogeneous yellow solution was transferred to a Teflon-lined stainless-steel autoclave and sealed to heat at 200 °C. After reaction for 10 h, the autoclave was cooled to room temperature. The obtained $Fe_3O_4$ microparticles were washed several times with ethanol and water, and then dried in vacuum for 12 h. The ratio of Na acrylate/NaOAc (w/w in gram) controls the grain size of the $Fe_3O_4$ particles. For example, the ratios of 1.5/0, 1.0/0.5, 0.5/1.0, 0.3/1.2, and 0.1/1.4 lead to the synthesis of $Fe_3O_4$ microparticles with average grain sizes of 5.9, 6.9, 8.3, 10.1, and 13.5 nm, respectively.

(6) Nam, J. M.; Thaxton, C. S.; Mirkin, C. A. *Science* **2003**, *301*, 1884–1886.
(7) Wilson, M. W.; Kerlan, R. K.; Fidelman, N. A.; Venook, A. P.; LaBerge, J. M.; Koda, J.; Gordon, R. L. *Radiology* **2004**, *230*, 287–293.
(8) Toprak, M. S.; McKenna, B. J.; Mikhaylova, M.; Waite, J. H.; Stucky, G. D. *Adv. Mater.* **2007**, *19*, 1362–1368.
(9) Euliss, L. E.; Grancharov, S. G.; O'Brien, S.; Deming, T. J.; Stucky, G. D.; Murray, C. B.; Held, G. A. *Nano Lett.* **2003**, *3*, 1489–1493.
(10) Bai, F.; Wang, D. S.; Huo, Z. Y.; Chen, W.; Liu, L. P.; Liang, X.; Chen, C.; Wang, X.; Peng, Q.; Li, Y. D. *Angew. Chem., Int. Ed.* **2007**, *46*, 6650–6653.
(11) (a) Zhuang, J. Q.; Wu, H. M.; Yang, Y. G.; Cao, Y. C. *J. Am. Chem. Soc.* **2007**, *129*, 14166–14167. (b) Zhuang, J. Q.; Wu, H. M.; Yang, Y. G.; Cao, Y. C. *Angew. Chem., Int. Ed.* **2008**, *47*, 2208–2212.
(12) (a) Hou, Y. L.; Gao, S.; Ohta, T.; Kondoh, H. *Eur. J. Inorg. Chem.* **2004**, *6*, 1169–1173. (b) Deng, H.; Li, X.; Peng, Q.; Wang, X.; Chen, J.; Li, Y. *Angew. Chem., Int. Ed.* **2005**, *44*, 2782–2845. (c) Zhu, Y.; Zhao, W.; Chen, H.; Shi, J. *J. Phys. Chem. C* **2007**, *111*, 5281–5285.
(13) Ge, J.; Hu, Y.; Biasini, M.; Beyermann, W. P.; Yin, Y. *Angew. Chem., Int. Ed.* **2007**, *46*, 4342–4345.
(14) (a) Tan, Y. W.; Zhuang, Z. B.; Peng, Q.; Li, Y. D. *Chem. Mater.* **2008**, *20*, 5029–5034. (b) Hu, X. L.; Gong, J. M.; Zhang, L. Z.; Yu, J. C. *Adv. Mater.* **2008**, *20*, 4845–4850.

**Synthesis of $Fe_3O_4$ Particles with Tunable Size of 6−170 nm.** $FeCl_3 \cdot 6H_2O$ (0.54 g), Na acrylate (1.5 g), NaOAc (1.5 g), were dissolved in a mixture of EG and DEG (total volume = 20 mL) under magnetic stirring. The obtained homogeneous yellow solution was transferred to a Teflon-lined stainless-steel autoclave and sealed to heat at 200 °C. After reaction for 10 h, the autoclave was cooled to room temperature. The obtained $Fe_3O_4$ particles were washed several times with ethanol and water, and then dried in vacuum for 12 h. The volume ratio of EG/DEG (v/v in mL) controls the size of the $Fe_3O_4$ particles. For example, the ratio of 0/20, 5/15, 10/10, and 20/0 lead to the synthesis of $Fe_3O_4$ particles with average sizes of 6, 60, 120, and 170 nm, respectively.

**Characterization.** X-ray powder diffraction patterns (XRD) of the products were obtained on a Japan Rigaku DMax-$\gamma$A rotation anode X-ray diffractometer equipped with graphite monochromatized Cu K$\alpha$ radiation ($\lambda$ = 1.54178 Å). Transmission electron microscopy (TEM) photographs were taken on a FEI CM120 microscope at an accelerating voltage of 120 kV and a high-resolution transmission electron microscope (HRTEM, JEOL-2010) at an accelerating voltage of 200 kV. Infrared (IR) spectra were recorded in the wavenumbers ranging from 4000 to 500 $cm^{-1}$ with a Nicolet model 759 Fourier transform infrared (FT-IR) spectrometer using a KBr wafer. Thermogravimetric analyses (TGA) were conducted with a Netzsch STA 409C thermo-analyzer instrument. The magnetic properties ($M-H$ curve) were measured at room temperature on a Lakeshore7300 magnetometer.

## 3. Results and Discussion

**3.1. Monodisperse $Fe_3O_4$ Microparticles with Tunable Grain Sizes.** Monodisperse $Fe_3O_4$ microparticles were synthesized by a modified solvothermal method. This unique approach provides the platform for the formation of primary $Fe_3O_4$ nanoparticles with tunable sizes and the simultaneous self-assembly of these nanograins into secondary monodisperse microparticles. Figure 1 shows the TEM images of the as-prepared monodisperse $Fe_3O_4$ microparticles. These particles are spherical and remarkably uniform with an average size about 280 nm (Figure 1a and b). Clearly, these microparticles are composed of small primary nanocrystals with a size of 5−7 nm (Figure 1c). The XRD patterns of the product (Figure 2a) can be indexed to face center cubic phase of $Fe_3O_4$ (JCPDS no. 19-0629). According to the Scherrer equation,[15] the average crystallite size which is calculated based on the XRD pattern (311), is approximately 5.9 nm, which agrees well with the TEM image. These monodisperse $Fe_3O_4$ microparticles can be well dispersed in water and diffract visible light upon the application of externally applied magnetic field (Figure 1d2). Also, the diffract color can be controlled by tuning the applied magnetic field strength (not shown), similar to the previous report by Yin et al.[16]

The growth of the $Fe_3O_4$ microparticles follows the well-documented two-stage growth model in which primary nanocrystals nucleate first in a supersaturated solution and then aggregate into larger secondary particles.[14b] Both the literature[12b,13,17] and our own experimental evidence have led us to believe that the coordinative ligand plays a crucial role in controlling the size of the primary nanocrystal nucleates. In order to obtain the monodisperse $Fe_3O_4$ microparticles with tunable grain sizes, we designed a modified synthetic route by controlling the ratios of Na acrylate/NaOAc (w/w). Figure 3 shows the representative TEM images of the as-prepared $Fe_3O_4$ microparticles, which are spherical with a narrow size distribution (~280 nm). These microparticles were synthesized by controlling the ratios (w/w) of Na acrylate/NaOAc from 1.5/0 (Figure 3a−c)

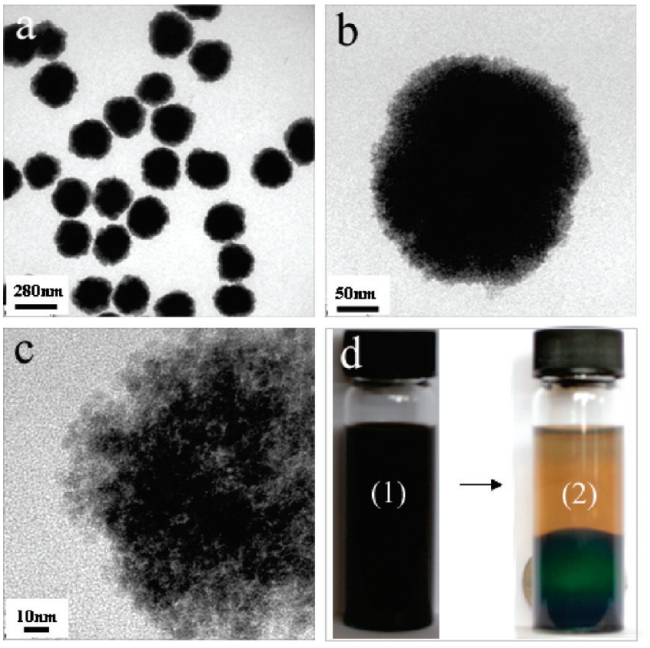


**Figure 1.** TEM images of the as-prepared monodisperse $Fe_3O_4$ microparticles, experimental parameters: [$FeCl_3 \cdot 6H_2O$] = 2 mmol, Na acrylate = 1.5 g, EG = 20 mL, temperature = 200 °C, and time = 10 h) (a,b,c) and photographs of an aqueous solution of $Fe_3O_4$ microparticles (d) without magnetic field (1) and with the externally applied magnetic field (2).

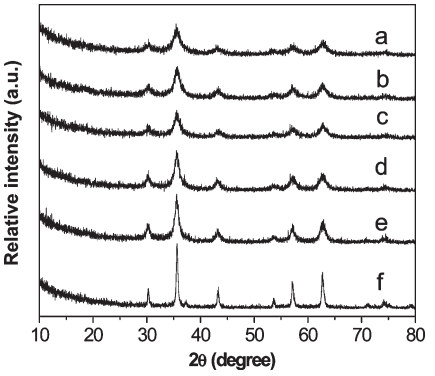


**Figure 2.** XRD patterns of the monodisperse $Fe_3O_4$ microparticles obtained using different amounts (gram) of Na acrylate/NaOAc (w/w): (a) 1.5/0, (b) 1.0/0.5, (c) 0.5/1.0, (d) 0.3/1.2, (e) 0.1/1.4, and (f) 0/1.5, with other experimental parameters kept constant ($FeCl_3 \cdot 6H_2O$ = 2 mmol, EG = 20 mL, temperature = 200 °C, and time = 10 h).

(15) Klug, H. P.; Alexander, L. E. *X-ray Diffraction Procedures for Polycrystalline and Amorphous Materials*; Wiley, New York, 1962, pp.491−538.
(16) (a) Ge, J.; Hu, Y.; Yin, Y. *Angew. Chem., Int. Ed.* **2007**, *46*, 7428–7431. (b) Ge, J.; Yin, Y. *Adv. Mater.* **2008**, *20*, 3485–3491.
(17) Lin, C. L.; Lee, C. F.; Chiu, W. Y. *J. Colloid Interface Sci.* **2005**, *291*, 411–420.

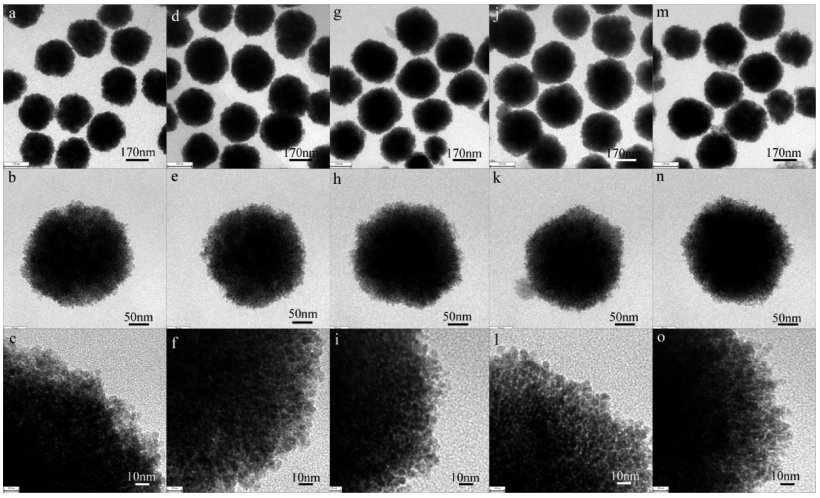


**Figure 3.** TEM images of the $Fe_3O_4$ microparticles obtained using different amounts (gram) of Na acrylate/NaOAc (w/w): (a−c) 1.5/0, (d−f) 1.0/0.5, (g−i) 0.5/1.0, (j−l) 0.3/1.2, and (m−o) 0.1/1.4, with other experimental parameters kept constant ($[FeCl_3 \cdot 6H_2O]$ = 2 mmol, EG = 20 mL, temperature = 200 °C, and time = 10 h).

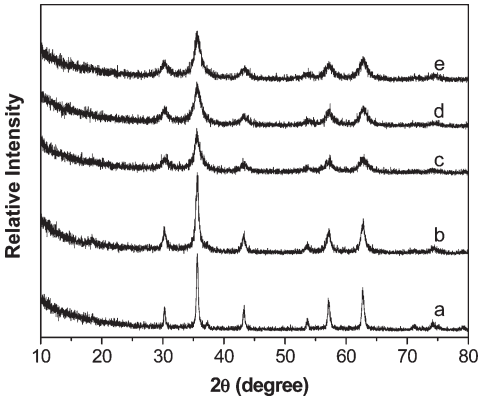


**Figure 4.** XRD patterns of the $Fe_3O_4$ microparticles obtained from the use of different amounts (gram) of Na acrylate: (a) 0, (b) 0.1, (c) 0.5, (d) 1.0, and (e) 1.5 with other experimental parameters kept constant ($[FeCl_3 \cdot 6H_2O]$ = 2 mmol, NaOAc = 1.5 g, EG = 20 mL, temperature = 200 °C, and time = 10 h).

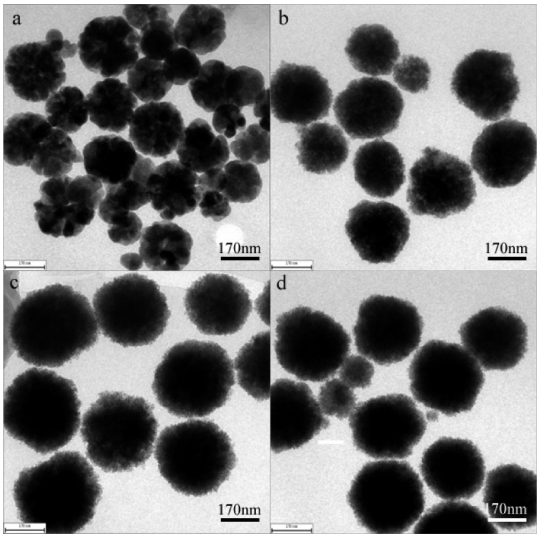


**Figure 5.** TEM images of the $Fe_3O_4$ microparticles obtained from the use of different amounts (gram) of Na acrylate: (a) 0, (b) 0.1, (c) 0.5, and (d) 1.0 with other experimental parameters kept constant ($[FeCl_3 \cdot 6H_2O]$ = 2 mmol, NaOAc = 1.5 g, EG = 20 mL, temperature = 200 °C, and time = 10 h).

to 1.0/0.5 (Figure 3d−f), 0.5/1.0 (Figure 3g−i), 0.3/1.2 (Figure 3j−l), and 0.1/1.4 (Figure 3m−o). The average sizes of the primary nanocrystals in the secondary $Fe_3O_4$ microparticles are increased from 5.9 to 6.9, 8.3, 10.1, and 13.5 nm, respectively, which were calculated by Scherrer equation from data of Figure 2. These results suggest that secondary structured $Fe_3O_4$ microparticles with continuously controlled grain sizes can be effectively synthesized via a simple one-step hydrothermal method. The average sizes of these primary $Fe_3O_4$ nanocrystals are smaller than the critical value $r_c$ (~20 nm),[13] which reveals that each primary nanocrystal is a single domain.

In this system, both NaOAc and Na acrylate play important roles in the formation of the superparamagnetic $Fe_3O_4$ microparticles with tunable grain sizes. NaOAc was selected to assist in the EG-mediated reduction of $FeCl_3$ into $Fe_3O_4$ by altering the alkalinity in the system.[12b,18] When the amount of Na acrylate is kept constant (0.5 g), the experiments evident that the grain sizes slightly increase (7.0, 7.2, 8.3, and 8.9 nm) with the gradual increase of pH, offered by the increasing amount of NaOAc (0, 0.5, 1.0, and 1.5 g) (Supporting Information (SI) Figure S1). These results agree that the hydrolysis rate of $FeCl_3$ accelerates by increasing alkalinity so as to promote the formation of larger particles.[13,18] However, when the amount of NaOAc is kept constant (1.5 g) in the mixture, the average grain sizes decrease from 21.5 to 15.5, 8.9, 8.0, and 7.5 nm with increasing amount of Na acrylate from 0 to 0.1, 0.5, 1.0, and 1.5 g (Figures 4 and 5). In this case, the grain sizes decrease with increasing alkalinity. Therefore, this result indicates that the Na acrylate acts as a stabilizer which can confine and stabilize the primary nanograins. Furthermore, $Fe_3O_4$ microparticles were synthesized by varying the Na acrylate content from 1.5 to 1.0 and 0.5 g in the absence of NaOAc

(18) Cao, S. W.; Zhu, Y. J.; Chang, J. *New J. Chem.* **2008**, *32*, 1526–1530.

**Scheme 1. Schematic Representation of the Formation of the Monodisperse $Fe_3O_4$ Microparticles with Tunable Grain Size and Particle Size**

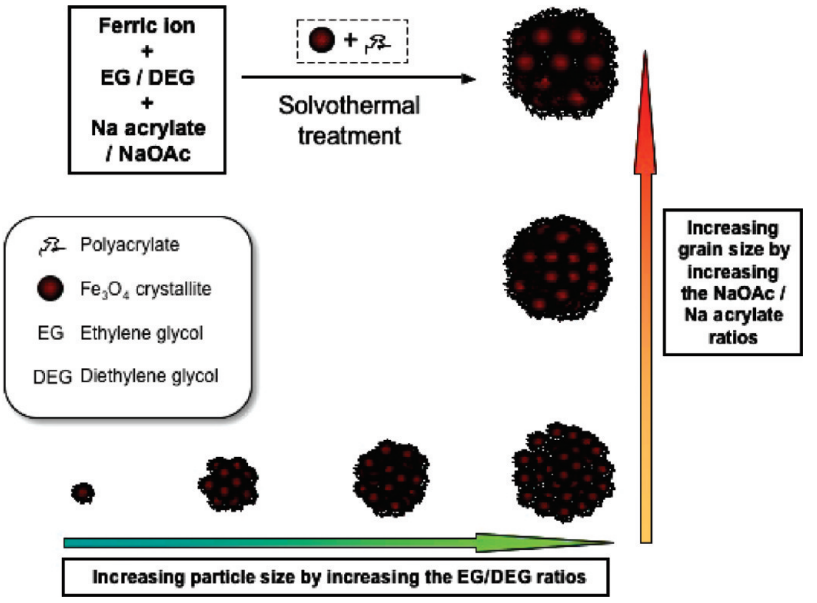


(SI Figure S2). Clearly, the grain sizes are slightly increased from 5.9 to 6.3 and 7.0 nm, which demonstrated that Na acrylate plays a significant role in controlling the size of the $Fe_3O_4$ nanograins. By adjusting the dosage of Na acrylate, the average grain size of the as-prepared superparamagnetic $Fe_3O_4$ microparticles can be controlled from 5.9 to 21.5 nm.

As a consequence, a proposed mechanism which leads to the resulting $Fe_3O_4$ microparticles with tunable grain sizes is shown in Scheme 1. In fact, when Na acrylate was introduced to the $FeCl_3$/EG solution, a significant amount of $Fe(OOCCH{=}CH_2)_3$ complex was formed. Then, in the presence of EG, the complex was transformed into $Fe_3O_4$ nucleates under hydrothermal treatment.[12b,18] Meanwhile, the freshly formed nanocrystals are unstable because they contain high surface energy, and thus they have a great tendency to aggregate rapidly.[14b] In previous reports,[13,14b] the average sizes of these nanograins almost similar no matter what the amounts of reagents or other reaction parameters change. However, in our system, variation of the concentration of Na acrylate will indeed change the particles' grain size. Because of the strong coordinations between iron(III) ions and carboxylate, the as-formed $Fe_3O_4$ nanograins also possessed a coating of Na acrylate. The acrylic double bonds in the coordinated Na acrylate on $Fe_3O_4$ nanograins and the uncoordinated Na acrylate in solution are activated by the iron ions, which further polymerize to give polyacrylate. The formed polyacrylate in situ would help stabilize the primary $Fe_3O_4$ nanograins, and confine them to form larger $Fe_3O_4$ grains in the recrystallization process.[17] By increasing the amount of Na acrylate, more polyacrylate will bind to the primary $Fe_3O_4$ nanocrystals' surface through the strong coordinating ligand. This results in a decrease of the size of $Fe_3O_4$ nanograins.[19] Consequently, the main driving force for the aggregation of nanograins is generally attributed to the reduced high surface energy through both the attachment among the primary nanoparticles and the polyacrylate which attached on the surface of the nanograins[20] Additionally, the grain size tunability may also be the result of slight differences in alkalinity caused by varying the amounts of NaOAc. The hydrolysis rate of $FeCl_3$ could be accelerated by increasing alkalinity so as to promote the formation of larger $Fe_3O_4$ nanocrystals, which was further supported by our experimental results. Moreover, the presence of water would also affect the grain size which can be applied from the above reasons.[18]

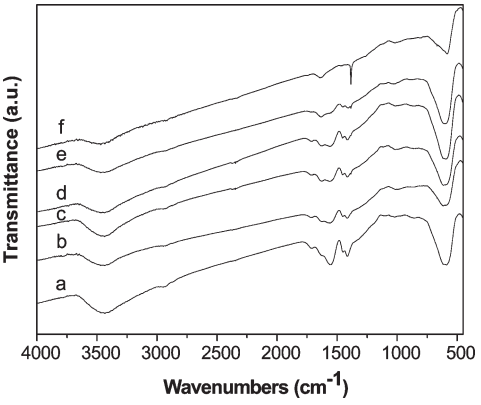


**Figure 6.** FTIR spectrum of the $Fe_3O_4$ microparticles obtained by the use of different amounts (gram) of Na acrylate/NaOAc (w/w): (a) 1.5/0, (b) 1.0/0.5, (c) 0.5/1.0, (d) 0.3/1.2, (e) 0.1/1.4, and (f) 0/1.5 with other experimental parameters kept constant ([$FeCl_3 \cdot 6H_2O$] = 2 mmol, EG = 20 mL, temperature = 200 °C, and time = 10 h).

In order to provide direct proofs for the presence of coordinative effect in the iron-carboxylate group, FTIR and TG characterizations were used. Figure 6 presents the

(19) Sun, X. H.; Zheng, C. M.; Zhang, F. X.; Li, L. D.; Yang, Y. L.; Wu, G. J.; Guan, N. J. *J. Phys. Chem. C* **2008**, *112*, 17148–17155.

(20) Chibowski, S.; Patkowski, J.; Grzadka, E. *J. Colloid Interface Sci.* **2009**, *329*, 1–20.

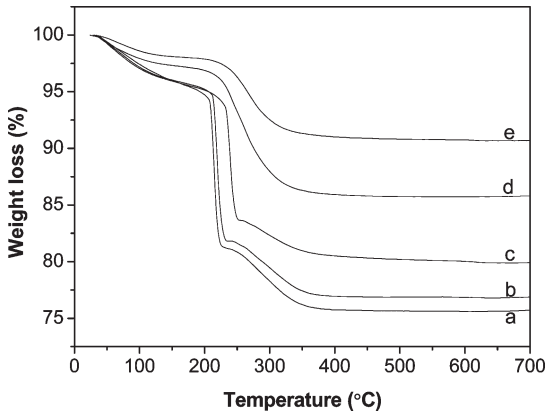


**Figure 7.** TG curves of the $Fe_3O_4$ microparticles obtained by the use of different amounts (gram) of Na acrylate/NaOAc (w/w): (a) 1.5/0, (b) 1.0/0.5, (c) 0.5/1.0, (d) 0.3/1.2, and (e) 0.1/1.4, with other experimental parameters kept constant ($[FeCl_3 \cdot 6H_2O]$ = 2 mmol, EG = 20 mL, temperature = 200 °C, and time = 10 h).

typical FTIR spectrum of the $Fe_3O_4$ microparticles with different grain sizes. The two peaks located at 1550 and 1405 $cm^{-1}$ are corresponded to the $COO^-$ antisymmetrical vibration and $COO^-$ symmetric vibration, indicating that large amounts of carboxylate groups are coordinated strongly to the iron cations.[13,17,21,22] Accordingly, the amounts of these functional groups decreased with the increase of grain size, which further proves that the $Fe_3O_4$ nucleates were sufficiently coordinated with Na acrylate. Similarly, TG results (Figure 7) also presents that higher organic compositions existed in the $Fe_3O_4$ microparticles with small nanograins than the ones with larger nanograins, an observation which agrees well with the proposed mechanism.

**3.2. Monodisperse $Fe_3O_4$ Particles with Tunable Particle Sizes.** There were only a few reports on the controllable synthesis of superparamagnetic $Fe_3O_4$ particles with size in the range of 5−200 nm. Previously, Li and his colleges[12b] have reported a general approach for the fabrication of monodisperse $Fe_3O_4$ microparticles by an EG solvothermal reduction method. The diameters of their products were influenced by reaction time and the concentration of starting materials, however, the sizes were tunable in the range of 200−800 nm. Although Yin's group[13] had recently reported a high-temperature hydrolysis method to grow monodisperse $Fe_3O_4$ nanoclusters with size from 30 to 180 nm, it is necessary to develop an efficient route for the synthesis of $Fe_3O_4$ particles with controllable sizes smaller than 200 nm.

Actually, in our EG-solvent system, if the amount of Na acrylate is kept constant (1.5 g) in the starting mixture, the sizes of as-prepared $Fe_3O_4$ particles slightly decreases from 280 to 240 and 170 nm (Figure 8a−c) with the amount of NaOAc increase from 0 to 1.0 and 1.5 g. However, when the amount of NaOAc is increased further, the size of as-prepared $Fe_3O_4$ particles has only a small decrease. Moreover, the $Fe_3O_4$ particle formation is a very rapid process: when the reaction time increased to 4 or 8 h, the product $Fe_3O_4$ particles possess a similar size. Therefore, it is very difficult to control the particle size from several to several hundreds nanometres by simply change the alkalinity or reaction time. These results demonstrate that many other methods should be employed to precisely control the size of $Fe_3O_4$ particles.

In this work, a novel bisolvent synthetic method was introduced to continuously control the sizes of $Fe_3O_4$ particles. During the reaction, EG play both roles as a reducing agent and a solvent during the formation of the $Fe_3O_4$ particles. Since the reaction temperature in the sealed container is 200 °C, which is slightly higher than the boiling point of EG (196 °C), therefore, EG may exist as a superfluid. At this temperature, $Fe_3O_4$ nanograins and polyacrylate assemble to form large secondary structural microparticles (Scheme 1). When DEG (boiling point = 240 °C) was introduced together with EG in the reaction system, quite surprisingly, the size of the $Fe_3O_4$ particles can be successfully reduced by only varying the EG/DEG ratio. Herein, control experiments using parameters for synthesis of 170 nm $Fe_3O_4$ particles ($FeCl_3 \cdot 6H_2O$ = 2 mmol, Na acrylate = 1.5 g, NaOAc = 1.5 g, temperature = 200 °C, and time = 10 h) were performed by changing the EG/DEG ratio. Figure 8a−d show the TEM images of as-prepared $Fe_3O_4$ particles, the size of the $Fe_3O_4$ particles significantly decreased while the amount of DEG increased. The diameters of the as-prepared $Fe_3O_4$ particles are ranging from 170 to 120, 60, and 6 nm when the EG/DEG ratio (v/v) changes from 20/0 to 10/10, 5/15, and 0/20.

Modifiers are very important for the synthesis of $Fe_3O_4$ particles with different size by using the bisolvent method. Besides the Na acrylate, poly(acrylic acid) (PAA) was also invited as the modifier to synthesis $Fe_3O_4$ particles. Figure 9a,b shows the SEM and TEM images of the $Fe_3O_4$ particles which synthesized in the presence of PAA. Obviously, the sizes of the $Fe_3O_4$ particles can also be successfully controlled to give the product with sizes of 180 and 100 nm when the EG/DEG ratios (v/v) were 20/0, and 5/15, respectively. In this bisolvent system, the polymer chain should have a strong affinity to the $Fe^{3+}$ ions. Figure 9c shows the TEM images of the $Fe_3O_4$ particles which were synthesized in the presence of PVP with the EG/DEG ratio (v/v) of 5/15. The average size of $Fe_3O_4$ nanoparticles is about 90 nm, which is much smaller than the products that were synthesized with an EG/DEG ratio of 20/0 (not shown). Clearly, PVP was also a proper modifier for the bisolvent method. As a comparison, if no Na acrylate, poly(acrylic acid) , and PVP were added to the reaction system, only random $Fe_3O_4$ nanoparticles with size about 10−30 nm were obtained when the EG/DEG ratio (v/v) was 5/15 (Figure 9d). Polyethylene glycol (6 kDa) and sodium citrate were also introduced into the reaction solution, however, the products were nonuniform nanoparticles (Figure 9e and f). Besides these linear polymers and small molecular modifiers in the synthesis, branched polyethylenimine (PEI) was also used. Interestingly, the formed products are porous

(21) Ge, J.; Hu, Y.; Biasini, M.; Dong, C.; Guo, J.; Beyermann, W. P.; Yin, Y. *Chem.—Eur. J.* **2007**, *13*, 7153–7161.
(22) Xuan, S. H.; Hao, L. Y.; Jiang, W. Q.; Gong, X. L.; Hu, Y.; Chen, Z. Y. *J. Magn. Magn. Mater.* **2007**, *308*, 210–213.

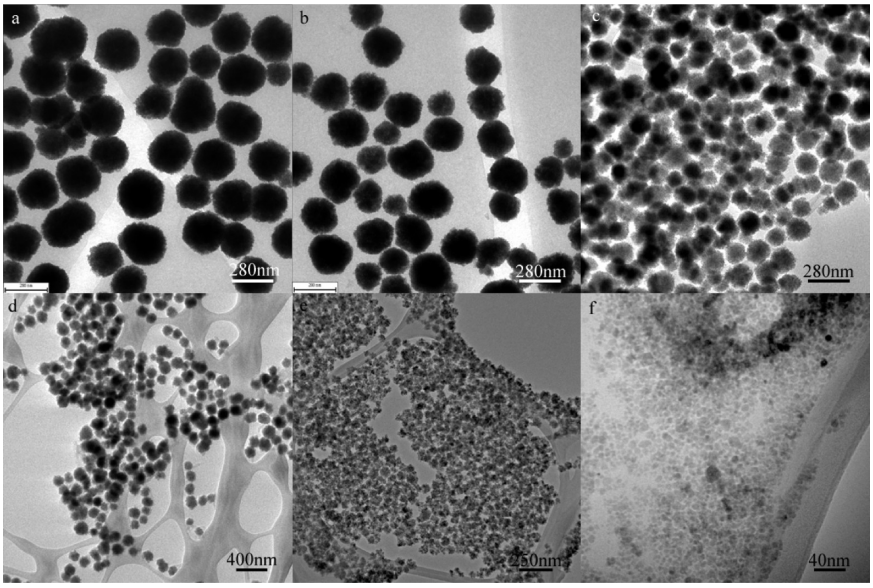


**Figure 8.** TEM images of the monodisperse $Fe_3O_4$ particles obtained using different amounts (gram) of Na acrylate/NaOAc (w/w): (a) 1.5/0, (b) 1.5/1.0, and (c) 1.5/1.5, with other experimental parameters kept constant. ($[FeCl_3 \cdot 6H_2O]$ = 2 mmol, EG = 20 mL, temperature = 200 °C, and time = 10 h); and TEM images of the monodisperse $Fe_3O_4$ particles obtained using different volume ratios (mL) of EG/DEG(v/v): (c) 20/0, (d) 10/10, (e) 5/15, and (f) 0/20, with other experimental parameters kept constant. ($[FeCl_3 \cdot 6H_2O]$ = 2 mmol, Na acrylate = 1.5 g, NaOAc = 1.5 g, temperature = 200 °C, and time = 10 h).

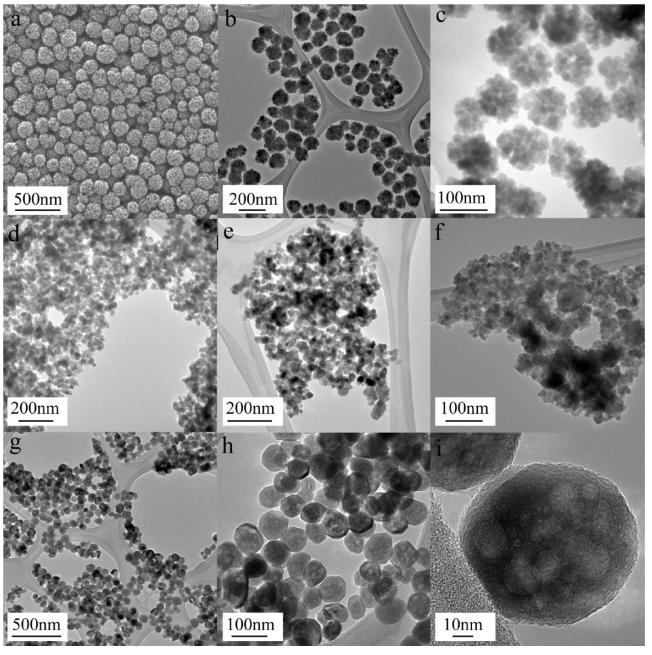


**Figure 9.** SEM and TEM images of the $Fe_3O_4$ particles obtained using PAA as the modifier with different EG/DEG ratios (v/v): (a) 20/0, and (b) 5/15; TEM images of the $Fe_3O_4$ particles obtained using PVP (c), no additives (d), PEG (e), sodium citrate (f) as the modifier while the EG/DEG ratios is 5/15; TEM images of the $Fe_3O_4$ particles obtained using PEI as the modifier (g−i). Other experimental parameters kept constant. ($[FeCl_3 \cdot 6H_2O]$ = 2 mmol, NaOAc = 1.5 g, temperature = 200 °C, and time = 10 h).

$Fe_3O_4$ nanoparticles, whereas the EG/DEG ratios did not influence the sizes of the porous nanoparticles (Figure 9g−i).

On the basis of the proposed mechanistic studies, we have identified two major characteristics: First, the $Fe_3O_4$ nanograins have strong affinity toward the polyacrylate chains via synergistic multidentate coordination and that they can assemble to form large secondary structural $Fe_3O_4$ microparticles. Most importantly, the size of these nanograins can be selectively obtained by tuning the concentration of the organic monomer (Na acrylate). With increasing concentration of Na acrylate, the average grain size of the $Fe_3O_4$ particle decreases. Second, the role of solvent is important to control the size of the secondary structure particles. When other parameters keep constant, the particle size decreases with increasing portion of DEG. As a result, 6−280 nm secondary structural $Fe_3O_4$ particles which are composed of different grain sizes (5.9−21.5 nm) can be selectively obtained by using our experimental procedures. On the other hand, eventually, other magnetic secondary structures with tunable particle sizes and grain sizes can also be prepared according to our procedures. This provides opportunities to study the property and relationships between grain size and particle size.

**3.3. Monodisperse $Fe_3O_4$ Microparticles with Grain Size-Dependent Magnetic Properties.** The unique and complex structures of the as-prepared monodisperse $Fe_3O_4$ microparticles which possess different grain sizes, allow them to retain superparamagnetic behavior at room temperature because the average grain size of these $Fe_3O_4$ microparticles is smaller than 20 nm.[13] In order to evaluate the magnetic response of the $Fe_3O_4$ microparticles to an externally applied magnetic field, the mass magnetization was measured at 300 K by cycling the field between −5 and 5 kOe. Figure 10 shows that all the monodisperse $Fe_3O_4$ microparticles with different grain sizes are superparamagnetic at room temperature. The saturation magnetization ($M_s$) values of the $Fe_3O_4$ particles were determined to be 36.2, 38.7, 46.5, and 67.2 emu/g whereas their grain sizes are 5.9, 6.9, 8.3, and 13.5 nm, respectively. By taking into account that these samples contain 26.9, 25.7, 22.8, 12.3% organic composition as

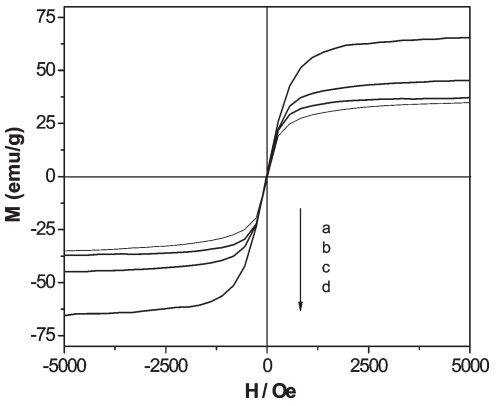


**Figure 10.** $M-H$ curves of the $Fe_3O_4$ microparticles with different average grain sizes: (a) 5.9, (b) 6.9, (c) 8.3, and (d) 13.5 nm.

polyacrylate according to the TG results (Figure 7), the $M_s$ values of the microparticles without organic composition are calculated as 49.5, 52.1, 60.2, and 76.8 emu/g, respectively (SI Figure S3) of pure $Fe_3O_4$. The saturation magnetization values of the products are smaller than that of the bulk $Fe_3O_4$ (92 emu/g), which most likely attributed to the much smaller size of the $Fe_3O_4$ primary nanocrystals and the existence of the organic fraction on surface.[22] The determined $M_s$ values for the $Fe_3O_4$ particles with small grain sizes are close, but they increase noticeably for the particles having larger nanograins. This observation is attributed to the large difference between the grain sizes and that it agrees well with the previous reports.[3a,14a,19]

Superparamagnetic $Fe_3O_4$ microparticles are prevalent in molecular imaging as the contrast agents for magnetic resonance imaging (MRI) due to their localized shortening of spin−spin ($T_2$) proton relaxation time.[23] In our work, the MRI properties of the as-prepared $Fe_3O_4$ microparticles with different grain sizes were also characterized. $T_2$ relaxometry which compares the relaxation rates between the $Fe_3O_4$ microparticles with grain sizes of 5.9, 10.1, and 13.5 nm are systematically investigated. The $Fe_3O_4$ microparticles with grain sizes 5.9, 10.1, and 13.5 nm yield $T_2$ relaxation rates of 65.3, 80.4, and 84.6 $s^{-1}mmol^{-1}$ Fe, respectively (SI Figure S4). From the results, the $Fe_3O_4$ microparticle with a large grain size (13.5 nm) yields a higher molar $T_2$ relaxation rate than the $Fe_3O_4$ microparticles with smaller grain size. The $r_2$ relaxivities of commercially available $Fe_3O_4$-based MRI contrast agents range from 33.4 for VSOP-C184 and 38 for Supravist to 120 for Feridex and 189 for Resovist.[24] It is well-known that the effects of crystallization nature of the $Fe_3O_4$ are related to the $T_2$ relaxation rate of the products.[23] Also, $r_2$ relaxivity of $Fe_3O_4$ particles is closely related to their particle size, and that larger particles tend to have higher $r_2$ relaxivity. The particle size of our $Fe_3O_4$ microparticles is close to that of VSOP-C184 and Supravist. From this aspect, because of the difference in crystallization nature, our microparticles demonstrate stronger relaxivity than VSOP-C184 and Supravist.

Furthermore, from the FTIR results, a weak band appeared at 1710 $cm^{-1}$ is attributed to the C=O stretching mode of the residue carboxylic acid groups,[21] which form complementary dimer pairs and sideway chains via hydrogen bonds (Figure 6a). This result indicates that there are still many polymer chains located on the micrometer-sized particles' surface with uncoordinated residue carboxylic acid groups. Therefore, the as-prepared monodisperse $Fe_3O_4$ microparticles with different grain sizes are very soluble in water. These microparticles are not only flexible building blocks with photonic properties (SI Figure S5), but also ideal candidates for the systematical study of their nanograin-dependent performance in optical, magnetic, catalytic, and biological applications. Because of the existence of large amounts of functional groups (e.g., —COOH) on the surface, the as-prepared $Fe_3O_4$ microparticles can be directly used as superparamagnetic spherical templates to fabricate well-defined core/shell structures without using any surface modification, which is necessary in other systems.[25] Based on this method, $Fe_3O_4$@$SiO_2$, $Fe_3O_4$@$TiO_2$ (SI Figure S6−10) and many other bifunctional core/shell composite particles can be successfully synthesized for many applications in magnetic separation, photocatalysis, or drug delivery.

## 4. Conclusions

In summary, a solvothermal process which utilizes controlled amounts of sodium acrylate, has been developed to synthesize a series of secondary structural $Fe_3O_4$ microparticles which are composed of small primary nanocrystals. The average nanograin size can be continuously tuned from 5.9 to about 21.5 nm by simply changing the weight ratios of Na acrylate/NaOAc. The as-prepared water-soluble $Fe_3O_4$ microparticles show superparamagnetic behavior at room temperature, and their saturation magnetization values correspond to the sizes of the $Fe_3O_4$ nanograins. With the increase of nanograins sizes, both $M_s$ and $T_2$ relaxation rate increase. Moreover, the size of the secondary structural $Fe_3O_4$ particles can also be precisely controlled from 6 to about 170 nm by using a novel bisolvent method. Therefore, the secondary structural $Fe_3O_4$ particles with different particle sizes and grain sizes can be selectively acquired by only varying the relative parameters. This work provides a new insight for the secondary nanostructure and also develops a new platform to study the property and relationships between grain size and particle size. More importantly, although this general method has been demonstrated using only $Fe_3O_4$ as the example, it is believed that this method can be extendible to construct secondary structures with other inorganic materials (such as ferrite, metal oxide) for specific functions. Additionally, such method also supply

(23) Larsen, B. A.; Haag, M. A.; Serkova, N. J.; Shroyer, K. R.; Stoldt, C. R. *Nanotechnology* **2008**, *19*(265102), 1–6.
(24) Corot, C.; Robert, P.; Idee, J.-M.; Port, M. *Adv. Drug Delivery Rev.* **2006**, *58*, 1471–1504.
(25) (a) Li, Y.; Wu, J.; Qi, D.; Xu, X.; Deng, C.; Yang, P.; Zhang, X. *Chem. Commun.* **2008**, *5*, 564–566. (b) Xu, X.; Deng, C.; Gao, M.; Yu, W.; Yang, P.; Zhang, X. *Adv. Mater.* **2006**, *18*, 3289–3293.

us an ideal magnetic template to direct the synthesis of magnetic bifunctional materials (such as $Fe_3O_4@SiO_2$ and $Fe_3O_4@TiO_2$, see the Supporting Information) without any additional surface modification on $Fe_3O_4$.

**Acknowledgment.** This work was supported by Direct Grants for Research (2060369 & 2041339) and also by a Strategic Investments Scheme from The Chinese University of Hong Kong as well as a General Research Fund (CUHK401709) from The Research Grants Council of Hong Kong.

**Supporting Information Available:** Experimental, XRD, MRI, FTIR, TEM, and EDX characterization data. This material is available free of charge via the Internet at http://pubs.acs.org.